ACS OMEGA

Open Access

http://pubs.acs.org/journal/acsodf

Article

The Long-Range Chromosomal Interaction Controlling Klotho Gene Expression in Human Chronic Kidney Disease

Pengwei Xu, Minjun Jiang, Jianchun Chen, Yongqiang Zhou, and Zhenfan Wang*

Cite This: *ACS Omega* 2024, 9, 51264−51270

Read Online

ACCESS | Metrics & More | Article Recommendations | Supporting Information

ABSTRACT: Cis-regulatory elements bridge enhancers and gene promoters to control gene expression via distal DNA interaction and three-dimensional chromosomal conformation organization. The aberrant changes of cis-acting regulatory systems as one type of the epigenetic regulative ways may be connected with human genetic diseases. Klotho, as an antiaging protein, is selectively expressed in kidney tissues and plays a crucial role in preventing chronic kidney disease (CKD) and renal fibrosis. However, the underlying transcription regulatory mechanism of Klotho in CKD is not fully understood. Herein, we analyzed the spatial organization of the chromatin region spanning 2 Mb upstream Klotho in human renal punctured CKD tissues using chromosome conformation capture (3C)-qPCR and identified the distal interaction of the Klotho promoter with certain specific chromatin regions characterized as the regulatory elements. Moreover, we determined that four DNase I hypersensitive sites (DHSs) involved in the regulation of Klotho gene expression lost their activities in CKD tissues compared to control accompanied by the reduction of H3K27ac. Finally, the CCCTC-binding factor (CTCF) sites were validated on the DHSs beyond the Klotho promoter by chromatin looping formation through the recruitment of CTCF.

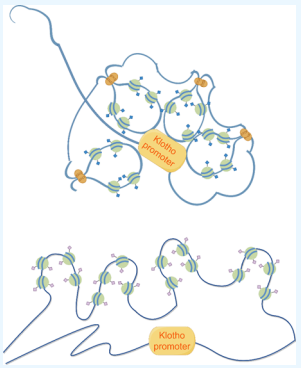

INTRODUCTION

Chronic kidney disease (CKD) is increasingly seen as a major public health problem associated with premature mortality with important social and economic implications. Over 10% of the global population suffers from this disease.[1] Klotho, predominantly expressed in renal tubules, is widely acknowledged to protect from inflammatory injury and renal fibrosis.[2] Klotho is remarkably reduced in the fibrotic kidneys of both patients with CKD and animal models.[3] Heterozygous Klotho deletion mice present with more severe renal fibrosis compared with the wild-type ones,[4] which confirms that the loss of Klotho could lead to the progression of renal fibrosis. On the other hand, rescuing Klotho by adding a recombinant Klotho protein or Klotho overexpression vector can compromise the progression of renal fibrosis *in vivo*.[5] Although the inhibitive effect and mechanisms of Klotho on CKD and renal fibrosis have been deeply illustrated, the reason why Klotho is downregulated during the progression of CKD has not been entirely understood.

One regulatory mechanism that controls gene transcription does rely on *cis*-regulatory sequences including enhancers and insulators usually situated far from the target genes.[6] The regulatory elements govern gene transcription through chromatin loop formation, allowing distal proximity between enhancers and gene promoters.[7] DNase I hypersensitive sites (DHSs) can help in characterizing accessible chromatin regions with activated transcription.[8] For that matter, variations in chromatin organization and alterations of remote interaction between *cis*-regulatory elements and target genes can both affect gene transcription and lead to progression of diseases, which is necessary and important for bridging between gene expression and genetic disorders.

In this study, the chromosomal architecture of Klotho and associated *cis*-regulatory elements were investigated in kidney tissues of patients with CKD using chromosome conformation capture (3C)-quantitative PCR (qPCR), and several DHSs associated with the regulation of Klotho gene expression were validated. Additionally, CCCTC-binding factor (CTCF) enrichments on Klotho were studied to determine the underlying mechanism of chromatin loop formation of Klotho in CKD.

MATERIALS AND METHODS

Sample Collection. Human renal tissues were obtained from nine patients with CKD and four patients with simple proteinuria by renal puncture biopsy from Suzhou Ninth People's Hospital during July 2021 to April 2022. Among the nine patients, CKD was derived from membranous nephropathy (MN) and mesangial proliferative nephritis (MPN) in four and five patients, respectively. Four patients with simple proteinuria were used as the negative control. The signed informed consent and ethics committee documents of the

Received: August 29, 2024
Revised: November 22, 2024
Accepted: December 2, 2024
Published: December 19, 2024

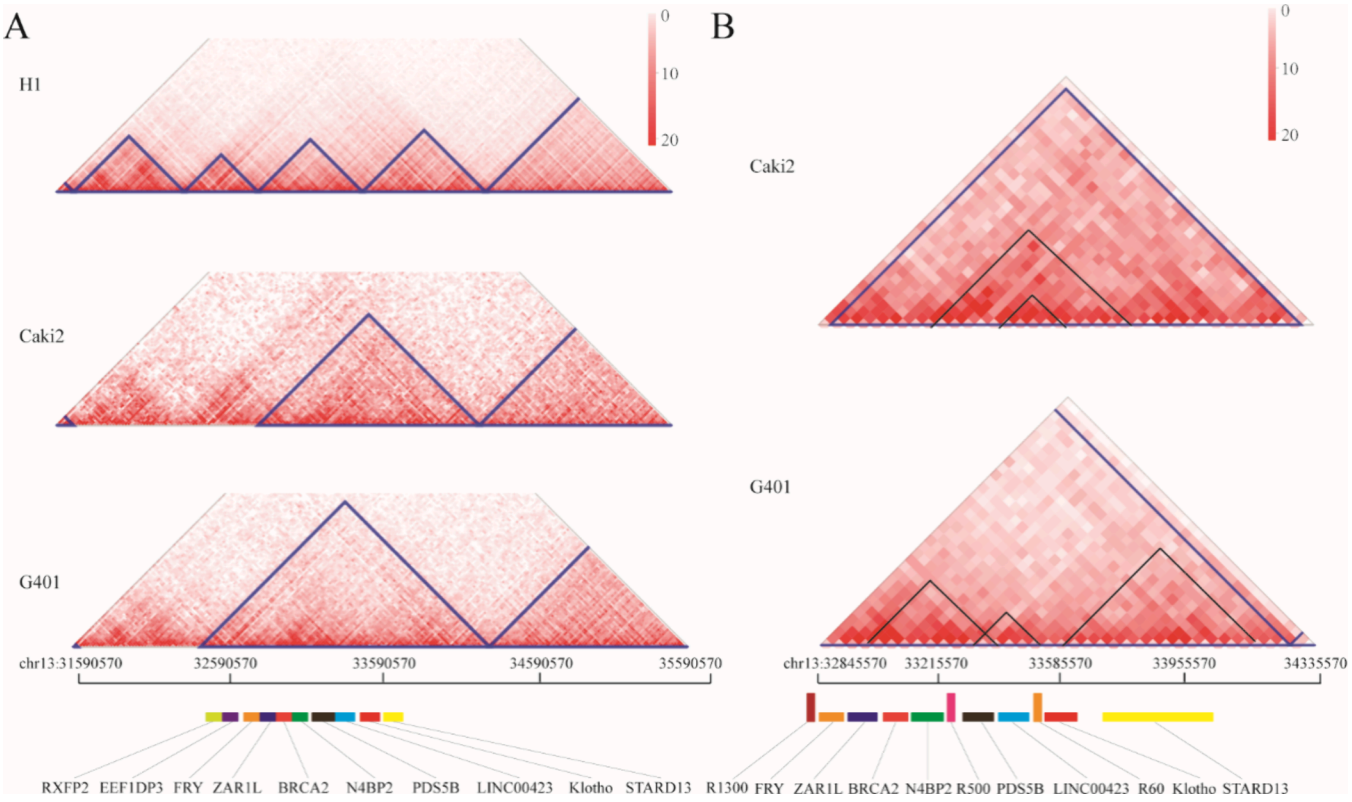

Figure 1. The chromosomal organization of Klotho. Heatmap generated by the 3DIV database in 2 Mb (A) and 40 Kb (B) resolution of the Hi-C study in the Klotho gene of H1 embryonic stem cells (top), Caki2 clear cell renal cell carcinoma cells (middle), and G401 renal carcinoma endothelial cells of hepatic sinusoid (bottom). Triangles represent putative TADs. Rectangles represent the gene and regulatory elements.

Ethics Committee of Suzhou Ninth People's Hospital were provided for study approval. Samples were rinsed thoroughly in ice-cold PBS and stored at −80 °C for next experiments.

Cell Culture. Renal proximal tubule epithelial (RPTEC) cells obtained from the Cell Bank of Shanghai Institutes of Biological Sciences, Chinese Academy of Sciences (Shanghai, China), which were grown in DMEM (Thermo Fisher Scientific, Waltham, MA, USA) with 10% FBS, were cultured at 37 °C in 5% CO2 saturated humid air.

Chromosome Conformation Capture (3C)-qPCR Assay. The 3C protocol was followed as previously described.[9] In brief, samples were fixed in 1.5% formaldehyde for 10 min and quenched by 0.125 M glycine for 5 min at room temperature (RT). Then, the samples were placed on ice and disrupted in lysis buffer [10 mM Tris (pH 8.0), 10 mM NaCl, 0.2% NP-40, supplemented with fresh protease inhibitor cocktail] for 10 min with a Dounce homogenizer (Kimble Chase Life Science and Research Products, Vineland, NJ, USA). Nuclei were harvested through 15,000 rpm centrifugation, washed twice, resuspended in 674 μL of 1× *Kpn*I buffer (NEB, Ipswich, MA, USA) and 76 μL of 1% SDS, and incubated for 10 min at 65 °C. To digest the mixture overnight, 400 U *Kpn*I was used, and the reaction was quenched by 88 μL of 10% Triton X-100. *Kpn*I was inactivated on the next day by adding 86 μL of 10% SDS and incubating the mixture for 30 min at 65 °C. Overall, 7.62 mL of ligation mix [750 μL of 10% Triton X-100, 750 μL of 10× ligation buffer, 80 μL of 10 mg/mL BSA, 80 μL of 100 mM ATP, and 3000 U T4 DNA ligase (NEB)] was prepared and incubated at 16 °C for 2 h. Libraries were treated with 45 μL of 10 mg/mL proteinase K (NEB) at 55 °C for 4 h, and DNA was purified with phenol−chloroform and used as a template for further qPCR assay.

Luciferase Assay. The individual DHSs combined with the 5′-flanking region (1500 bp) of the Klotho gene, defined as the Klotho promoter, were cloned into the upstream of luciferase cDNA of the pGL3-basic vector (Promega, Madison, WI, USA) at *Kpn*I and *Hin*dIII sites. pGL3-basic and pGL-3 with the Klotho promoter were used as controls. RPTEC cells at a density of 1×10^6 were subcultured in 6-well plates. Transfections were performed using lipofectamine (Thermo Fisher Scientific) when the cells attached to the plate. At 48 h after transfection, the cells were washed with 1× PBS twice and lysed with lysis buffer (Promega). Supernatants of the cell lysate were harvested by centrifugation at 15,000 *g* for 5 min at 4 °C. A total of 20 μL of each lysate was used to assess the luciferase activity. Promega reagents and a multiwall plate reader Varioskan (Thermo Fisher Scientific) were used. The data were presented as relative Klotho transcription activity driven by the DHSs.

Chromatin Immunoprecipitation Assay. The procedures of tissue cross-linking and cell breaking were the same with 3C as described above. Genomic DNA of the samples was sonicated to shear into 200−300 bp as per the following conditions: 5 s high power and 30 s interval for 40 cycles (Bioruptor Pico 60 kHz, Diagenode, Seraing, Belgium). Of the total cell lysate, 10% was stored as the input, and the rest was incubated with 1 μg CTCF or H3K27ac antibodies (Abcam, Cambridge, MA, USA) at 4 °C overnight and pulled down by protein-A beads (Thermo Fisher Scientific) for 2 h at 4 °C.

DNase I Assay. The procedures of cell cross-linking and cell breaking were the same with 3C as described above. A

https://doi.org/10.1021/acsomega.4c07967
ACS Omega 2024, 9, 51264−51270

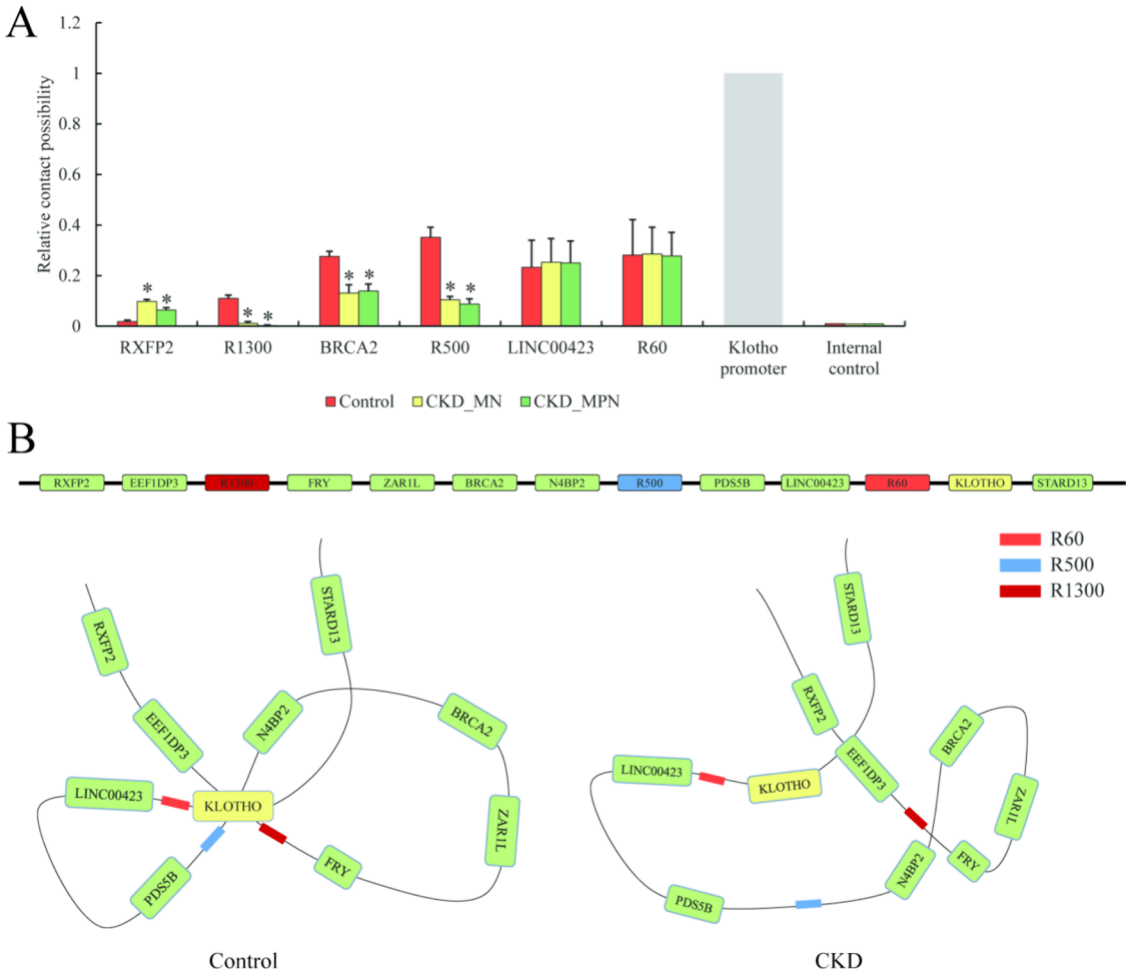

Figure 2. The long-range interaction between Klotho promoter and other regions. 3C-qPCR for the interaction between the Klotho promoter and nearby genes or regulatory elements (A). Control, CKD_MN, and CKD_MPN refer to the samples of proteinuria, membranous nephropathy, and mesangial proliferative nephritis, respectively. The 3C-qPCR data are presented as mean ± SEM of triplicate biological replicates. "*" represents the contact possibility of the Klotho promoter to the corresponding targets with $p < 0.05$ by Student's t test. The putative diagram of Klotho DNA-looping alteration from the control to CKD according the 3C-qPCR results (B). Red, blue, and brown rectangles represent R60, R500, and R1300 regions, respectively, which are of our interest in this study.

total of 5 μg genomic DNA was quantified and digested by 1 U DNase I (NEB) at 37 °C for 1 h. DNA was purified with phenol−chloroform and used as a template for further qPCR assay.

qPCR Assay. For qPCR, 1 μL of template DNA was taken and the QuantStudio 3 system (Thermo Fisher Scientific) was used. In accordance with the given instructions, the PCR conditions were as follows: 95 °C for 30 s for initial denaturation, followed by 40 cycles at 95 °C for 5 s, appropriate annealing temperatures of 10 s and 72 °C, then 30 s. Ct values were harvested and calculated using the 2^delta−delta method. Tubulin was used as an internal control, as previously described,[10] for the 3C assay. Sequences of all primers used in this study are listed in Supplementary Table 1.

Statistical Analysis. The data were presented as means ± SEM. All statistical analyses were performed using SPSS 20 software (IBM, Armonk, NY, USA). Student's t-test was used to evaluate the difference among groups. A p value of less than 0.05 was considered statistically significant.

RESULTS

Long-Distance Interactions between the Enhancer Element and Klotho Promoter. To date, very few studies have determined the mechanisms underlying the control of Klotho transcription by long-range regulatory elements. To decipher the probable genomic spatial interactions around the Klotho promoter (chr13:33016423−33066143 according to GRCh38, the same below) and corresponding domains for regulating Klotho expression, we investigated the potential distal and proximal interactions of Klotho using public 3C data (Hi-C) from the 3DIV database (http://kobic.kr/3div/).[11] Hi-C, as a novel high-throughput technique allowing the genome-wide quantification of chromosomal interactions in cell populations, displays the chromosomal organization via topologically associating domains (TADs) corresponding to regions enriched in chromatin contacts. Given the comparative interaction visualization, we observed the overall pattern of the DNA distal interaction at Klotho in H1 embryonic stem cells, Caki2 clear cell renal cell carcinoma cells, and G401 renal carcinoma cells. The different TADs could be identified across embryonic stem cells and kidney cancers. We observed that Klotho was located at the boundary of two individual TADs in

https://doi.org/10.1021/acsomega.4c07967
ACS Omega 2024, 9, 51264−51270

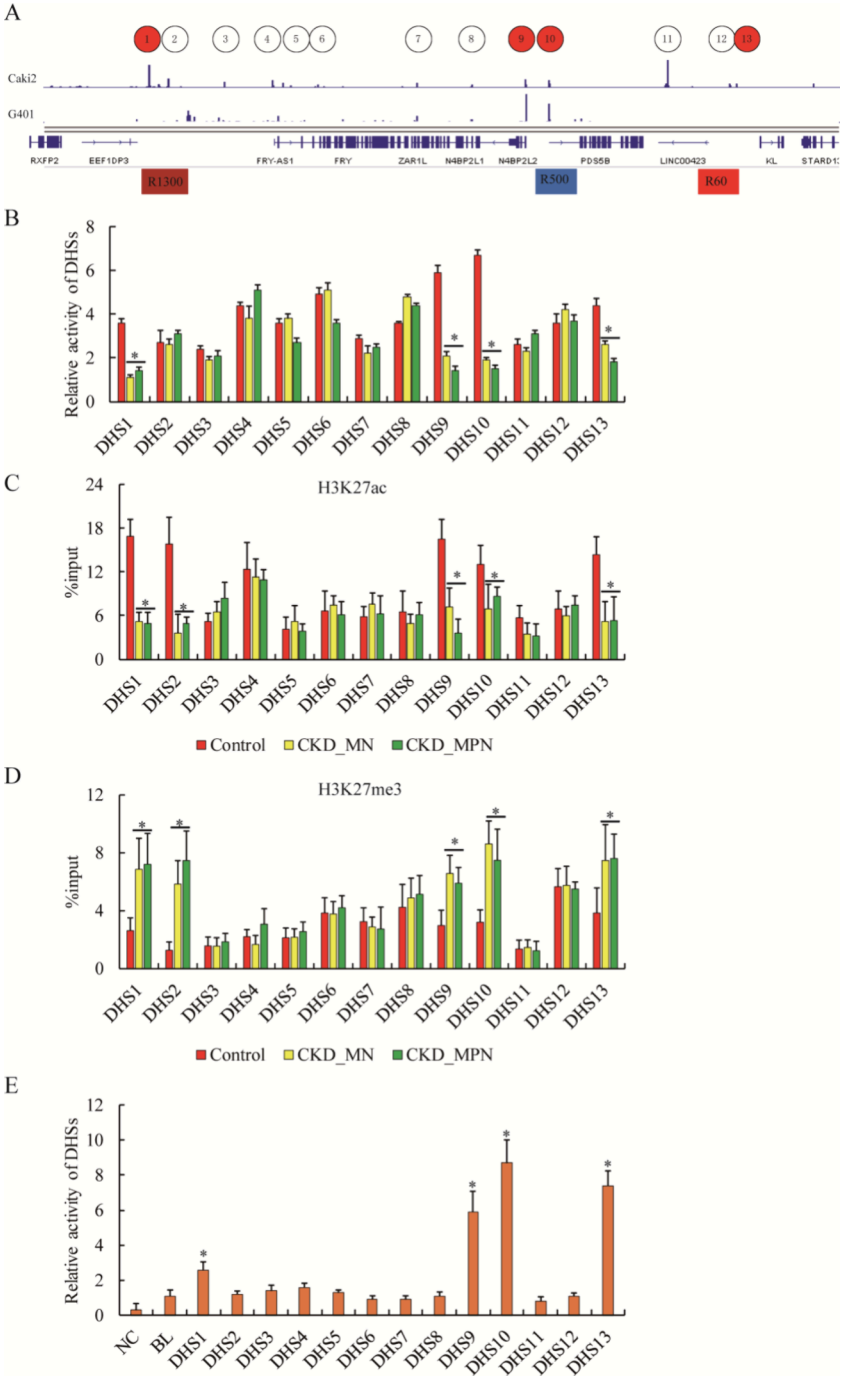

Figure 3. DHSs distribution around Klotho. DNase-seq data of Caki2 and G401 cells from the ENCODE database (A). Total 13 DHSs located within R60, R500, and R1300 are labeled with numbers. Numbers 1, 9, 10, and 13 DHSs having enhancer activities are highlighted in red.

H1 embryonic stem cells but at the center of one substantial TAD in Caki2k or G401 kidney-specific cells (Figure 1A), which indicated that the chromosomal environment of Klotho is likely to be similar in renal-specific cells or tissues. Additionally, the TAD in kidney cancer cells, whose 5′ boundary is situated 1.3 Mb upstream from the Klotho coding region (chr13:31979886−32010674; R1300 for short, the same below), and the sub-TADs in Caki2 and G401 cells, whose 5′ boundary is approximately 500 kb (chr13:32511726−32593341; R500) and 60 kb (chr13:32952127−32972341; R60) upstream from the Klotho gene, respectively, were observed under the higher resolution of heatmap (Figure 1B). Taken together, the Hi-C data provided the basic information on the genomic environment around the Klotho gene and implied a complicated chromosomal architecture for regulating Klotho transcription in kidney tissues.

Spatial Chromosomal Organization of Klotho in CKD Tissues. Considering three regions interacting with Klotho from Hi-C data of renal cancer cells, the detailed chromatin organization in CKD had to be validated. We mapped the interaction profile of the Klotho promoter with R60, R500, and R1300 in CKD and control samples using 3C-qPCR (Figure 2A). The overall presence of the chromosomal architecture of

https://doi.org/10.1021/acsomega.4c07967
ACS Omega 2024, 9, 51264−51270

the Klotho promoter captured from those three regions was observed to be seemingly similar. Interactions between the Klotho promoter and R60 as well as LINC00423 were preferentially found in all the samples, and these were the highest contacts compared with the other regions. Interactions of the Klotho promoter with R500 and BRCA2 significantly weakened in CKD compared with the control. On the contrary, the genomic interactions of RXFP2 with Klotho both strengthened in CKD compared with the control. Unexpectedly, the interactions of Klotho with R1300 were almost completely lost in CKD. R1300 was considered to be a TAD boundary from the aforementioned Hi-C data, which indicated that the TAD where Klotho was located might undergo a putative reorganization in CKD (Figure 2B). Taken together, these results suggest that several putative regulatory elements contribute to Klotho transcription regulation through physical proximity with the Klotho promoter.

Regulatory Activities of DHSs for Klotho Transcription. One common type of regulatory element is nucleosome-free DHSs, which can be recruited by multiple *cis*-regulatory factors. To search and evaluate functional DHSs around Klotho in CKD, we aligned available DNase-seq data of Caki2 (ENCSR515EWI) and G401 (ENCSR269SIA) from the ENCODE database (https://www.encodeproject.org)[12] along the Klotho gene (Figure 3A). Total 13 DHS fragments having potential enhancer activities (six DHSs majorly located in R60, R500, and R1300) were observed. These DHSs were selected to conduct DNase-qPCR for investigating the activity of the clinical samples. We observed that four DHSs encompassing chr13:31,742,215−31,742,365; chr13:32,538,815−32,538,965; chr13:32,586,315−32,586,465; and chr13:32,911,615−32,911,785, which all were distributed in the R60, R500, and R1300 regions, lost their activities in CKD tissues compared with the control, whereas other DHSs displayed no significant difference among these samples in our study (Figure 3B). Meanwhile, the enrichment of H3K27ac was used to validate the activity of DHSs. Compromised H3K27ac modifications on DHSs, including DHS1, DHS2, DHS9, DHS10, and DHS13, were observed in CKD (Figure 3C). Consistently, the enrichments of enhancer repressive mark H3K27me3 on DHS1, DHS2, DHS9, DHS10 and DHS13 were opposite to H3K27ac (Figure 3D). Furthermore, an *in vitro* reporter assay was used to detect the enhancer activities of these four DHSs against the Klotho promoter. The pGL3 vectors with each DHS linked with the Klotho promoter and modified firefly luciferase were individually cotransfected into RPTEC cells, in which Klotho was highly expressed.[13] The luciferase signals were normalized against the Klotho promoter construct alone. Consistently, these four DHS fragments significantly enhanced Klotho promoter activity, whereas the other DHSs did not show any enhancer activity in RPTEC cells (Figure 3E). Altogether, our results indicated that several DHSs played an important role in controlling Klotho transcription regulation in CKD.

The activity of DHSs in CKD using the DNase-qPCR assay (B). The enrichment of H3K27ac (C) and H3K27me3 (D) of different DHSs for the Klotho promoter in RPTEC cells using ChIP-qPCR. The enhancer activities of different DHSs for the Klotho promoter in RPTEC cells using the luciferase reporter assay (E). NC, BL, and DHS, respectively, refer to pGL3-basic, pGL3 with the Klotho promoter, and pGL3 with the corresponding DHS and Klotho promoter. qPCR data are presented as mean ± SEM of triplicate biological replicates. "*" represents $p < 0.05$ vs. control or NC and BL by Student's t test.

Alteration of CTCF Enrichment around DHSs in CKD. Finally, the underlying mechanism of chromosomal architecture alteration at Klotho in CKD is revealed. Usually, CTCF exerts genome architectural organization by creating local chromatin hubs, joining clusters of genes, and enhancing the connection between regulatory elements and the corresponding promoters.[12] CTCF enrichment largely varies across different cell types or pathogenesis. Therefore, DHSs are involved in the formation of a chromatin loop at the Klotho gene because of CTCF recruitment or dissociation. Chromatin immunoprecipitation (ChIP)-qPCR was conducted, and reduced CTCF enrichment at R1300 and R500 involving DHS1, DHS2, DHS9, and DHS10 was observed in CKD as against the control (Figure 4). Collectively, we determined that aberrant CTCF binding might connect with chromosomal organization and dysregulation of Klotho transcription in CKD.

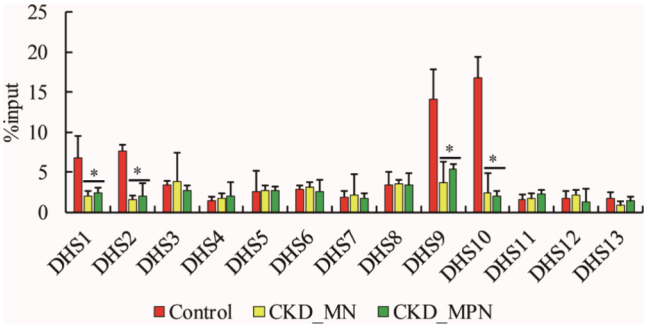

Figure 4. The CTCF enrichment on DHSs in CKD. ChIP-qPCR data are presented as mean ± SEM of triplicate biological replicates. "*" represents $p < 0.05$ vs. control by Student's t test.

DISCUSSION

CKD is a progressive systemic disease that irreversibly changes the structure and function of the kidney. Additionally, CKD progression can have multiple negative systemic effects on numerous organs. Growing evidence suggests that a reduced Klotho, initially principally described as an antiaging gene, contributes to the development and progression of CKD.[14] The Klotho gene is highly expressed in the cell surface membranes of proximal and distal renal tubules, which are majorly maintained by the kidney under the normal physiological conditions. Previous studies have reported that Klotho happens to decline, along with renal insufficiency, in individuals or animal models with CKD.[15] Nevertheless, Klotho is highly related to the pathogenic mechanism of CKD and is considered as a hallmark as well as a potential therapeutic target for CKD.

The chromosomal architecture around Klotho is beneficial to characterize the underlying alternative regulatory effect of Klotho transcription and may give the epigenetic reasons behind some cases of CKD without any aberrant genotype. Usually, the overall chromosomal architecture including compartment A/B distribution and TAD organization presents a cell- or tissue-specific landscape.[16] Therefore, the renal-cell-specific Hi-C data were employed to characterize the rough chromatin environment around Klotho, and the basic regulatory elements were revealed despite some minor

https://doi.org/10.1021/acsomega.4c07967
ACS Omega 2024, 9, 51264−51270

variations among the cell samples (Figure 1). Klotho is supposed to be situated in the center of one TAD in the kidney. The robust interacting regions correlating with the regulatory elements R60 and R500 are all located within the Klotho sub-TAD, whereas R1300 is located near the boundary region of sub-TAD. Our 3C results showed that R1300 and R500 reduce the distal interaction with Klotho, particularly in CKD (Figure 2), which indicates that the sub-TAD of Klotho undergoes reorganization and the epigenetic environment for Klotho transcription activity changes when CKD occurs.

Moreover, luciferase expression driven by a Klotho promoter fragment suggests that four DHSs play a regulatory role in Klotho transcription, but they lose the phenotype of enhancer activities along with the altered chromosomal organization in CKD. The possible reason is that the altered chromosomal architecture breaks off the distal connection between DHSs and the Klotho promoter; meanwhile, the epigenetic pattern of DHSs, such as histone or DNA methylation modification, allows the heterochromatin status for transcriptional suppression in CKD. Nevertheless, further explanation on the dynamic change in transcription factors binding to these DHSs in CKD is not provided in this study.

The accompanied alteration of CTCF enrichment around Klotho provides insights into the aberrant chromosomal organization in CKD. Combined with 3C results, the loss of CTCF at DHS1, DHS2, DHS9, and DHS10 is supposed to eliminate the interval among DNA loops, creating an environment for the equal transcriptional activity of Klotho and other nearby genes. This indicates that CTCF-mediated chromatin looping can determine the coordination of *cis*-acting regulatory elements for gene transcription. However, no change in CTCF-binding affinities from DHS3 to DHS8 between CKD and the control suggests a stable DNA looping within R500 to R1300. Nevertheless, the observation that CTCF binding is lowered in CKD could be an effect of the disease but not a necessary cause. The regional CTCF enrichment is supposed to be impacted by multiple factors including the transcription factor interaction, genomic variation, or mutual attraction among CTCF proteins, which needs to be further investigated in CKD.

CONCLUSIONS

We identified four DHSs surrounding the Klotho gene that substantially affected Klotho expression through their interaction with the promoter in CKD tissues. We propose a 3D DNA-looping model in the chromosomal organization of the Klotho locus in human CKD tissues via formation of a chromatin loop, which depended on CTCF recruitment. Our novel discovery can provide the mechanisms underlying molecular pathogenesis of CKD.

ASSOCIATED CONTENT

Supporting Information

The Supporting Information is available free of charge at https://pubs.acs.org/doi/10.1021/acsomega.4c07967.

Primer sequence used in this study (PDF)

AUTHOR INFORMATION

Corresponding Author

Zhenfan Wang − *Department of Urology, Suzhou Ninth Hospital affiliated to Soochow University, Suzhou 215000, China*; orcid.org/0009-0003-0097-2301; Phone: +86-0512-82881250; Email: Wangzf028@126.com

Authors

Pengwei Xu − *Department of Urology, Suzhou Ninth Hospital affiliated to Soochow University, Suzhou 215000, China*

Minjun Jiang − *Department of Urology, Suzhou Ninth Hospital affiliated to Soochow University, Suzhou 215000, China*

Jianchun Chen − *Department of Urology, Suzhou Ninth Hospital affiliated to Soochow University, Suzhou 215000, China*

Yongqiang Zhou − *Department of Urology, Suzhou Ninth Hospital affiliated to Soochow University, Suzhou 215000, China*

Complete contact information is available at: https://pubs.acs.org/10.1021/acsomega.4c07967

Notes

The authors declare no competing financial interest.

ACKNOWLEDGMENTS

The project is financially supported by the Science and Technology Development Plan Program of Suzhou (SKYD2023072).

REFERENCES

(1) Luo, S.; Grams, M. E. Epidemiology research to foster improvement in chronic kidney disease care. *Kidney Int.* **2020**, *97*, 477.

(2) Satoh, M.; Nagasu, H.; Morita, Y.; Yamaguchi, T. P.; Kanwar, Y. S.; Kashihara, N. Klotho protects against mouse renal fibrosis by inhibiting Wnt signaling. *Am. J. Physiol Renal Physiol* **2012**, *303* (12), F1641−1651. Liu, Q. F.; Ye, J. M.; Yu, L. X.; Dong, X. H.; Feng, J. H.; Xiong, Y.; Gu, X. X.; Li, S. S. Klotho mitigates cyclosporine A (CsA)-induced epithelial-mesenchymal transition (EMT) and renal fibrosis in rats. *Int. Urol Nephrol* **2017**, *49* (2), 345−352.

(3) Zhou, L.; Li, Y.; Zhou, D.; Tan, R. J.; Liu, Y. Loss of Klotho contributes to kidney injury by derepression of Wnt/beta-catenin signaling. *J. Am. Soc. Nephrol* **2013**, *24* (5), 771−785. Koh, N.; Fujimori, T.; Nishiguchi, S.; Tamori, A.; Shiomi, S.; Nakatani, T.; Sugimura, K.; Kishimoto, T.; Kinoshita, S.; Kuroki, T.; et al. Severely reduced production of klotho in human chronic renal failure kidney. *Biochem. Biophys. Res. Commun.* **2001**, *280* (4), 1015−1020.

(4) Sugiura, H.; Yoshida, T.; Shiohira, S.; Kohei, J.; Mitobe, M.; Kurosu, H.; Kuro-o, M.; Nitta, K.; Tsuchiya, K. Reduced Klotho expression level in kidney aggravates renal interstitial fibrosis. *Am. J. Physiol Renal Physiol* **2012**, *302* (10), F1252−1264.

(5) Chen, T. H.; Kuro, O. M.; Chen, C. H.; Sue, Y. M.; Chen, Y. C.; Wu, H. H.; Cheng, C. Y. The secreted Klotho protein restores phosphate retention and suppresses accelerated aging in Klotho mutant mice. *Eur. J. Pharmacol.* **2013**, *698* (1−3), 67−73. Guan, X.; Nie, L.; He, T.; Yang, K.; Xiao, T.; Wang, S.; Huang, Y.; Zhang, J.; Wang, J.; Sharma, K.; et al. Klotho suppresses renal tubulo-interstitial fibrosis by controlling basic fibroblast growth factor-2 signalling. *J. Pathol* **2014**, *234* (4), 560−572.

(6) Kleinjan, D. A.; van Heyningen, V. Long-range control of gene expression: emerging mechanisms and disruption in disease. *Am. J. Hum. Genet.* **2005**, *76* (1), 8−32. Dekker, J. Gene regulation in the third dimension. *Science* **2008**, *319* (5871), 1793−1794.

(7) Zhang, Y.; Wong, C. H.; Birnbaum, R. Y.; Li, G.; Favaro, R.; Ngan, C. Y.; Lim, J.; Tai, E.; Poh, H. M.; Wong, E.; et al. Chromatin connectivity maps reveal dynamic promoter-enhancer long-range associations. *Nature* **2013**, *504* (7479), 306−310.

(8) Lyu, C.; Wang, L.; Zhang, J. Deep learning for DNase I hypersensitive sites identification. *BMC Genomics* **2018**, *19* (Suppl 10), 905.
(9) Moisan, S.; Levon, S.; Cornec-Le Gall, E.; Le Meur, Y.; Audrezet, M. P.; Dostie, J.; Ferec, C. Novel long-range regulatory mechanisms controlling PKD2 gene expression. *BMC Genomics* **2018**, *19* (1), 515.
(10) Hou, C.; Dale, R.; Dean, A. Cell type specificity of chromatin organization mediated by CTCF and cohesin. *Proc. Natl. Acad. Sci. U.S.A.* **2010**, *107* (8), 3651−3656.
(11) Yang, D.; Jang, I.; Choi, J.; Kim, M. S.; Lee, A. J.; Kim, H.; Eom, J.; Kim, D.; Jung, I.; Lee, B. 3DIV: A 3D-genome Interaction Viewer and database. *Nucleic Acids Res.* **2018**, *46* (D1), D52−D57.
(12) Davis, C. A.; Hitz, B. C.; Sloan, C. A.; Chan, E. T.; Davidson, J. M.; Gabdank, I.; Hilton, J. A.; Jain, K.; Baymuradov, U. K.; Narayanan, A. K.; et al. The Encyclopedia of DNA elements (ENCODE): data portal update. *Nucleic Acids Res.* **2018**, *46* (D1), D794−D801.
(13) Erben, R. G.; Andrukhova, O. FGF23-Klotho signaling axis in the kidney. *Bone* **2017**, *100*, 62−68.
(14) Hu, M. C.; Kuro-o, M.; Moe, O. W. Klotho and chronic kidney disease. *Contrib. Nephrol.* **2013**, *180*, 47−63. Lindberg, K.; Amin, R.; Moe, O. W.; Hu, M. C.; Erben, R. G.; Ostman Wernerson, A.; Lanske, B.; Olauson, H.; Larsson, T. E. The kidney is the principal organ mediating klotho effects. *J. Am. Soc. Nephrol* **2014**, *25* (10), 2169−2175.
(15) Hu, M. C.; Shi, M.; Zhang, J.; Quinones, H.; Griffith, C.; Kuro-o, M.; Moe, O. W. Klotho deficiency causes vascular calcification in chronic kidney disease. *J. Am. Soc. Nephrol* **2011**, *22* (1), 124−136. Lau, W. L.; Leaf, E. M.; Hu, M. C.; Takeno, M. M.; Kuro-o, M.; Moe, O. W.; Giachelli, C. M. Vitamin D receptor agonists increase klotho and osteopontin while decreasing aortic calcification in mice with chronic kidney disease fed a high phosphate diet. *Kidney Int.* **2012**, *82* (12), 1261−1270.
(16) Paulsen, J.; Liyakat Ali, T. M.; Nekrasov, M.; Delbarre, E.; Baudement, M. O.; Kurscheid, S.; Tremethick, D.; Collas, P. Long-range interactions between topologically associating domains shape the four-dimensional genome during differentiation. *Nat. Genet.* **2019**, *51* (5), 835−843.

https://doi.org/10.1021/acsomega.4c07967
ACS Omega 2024, 9, 51264−51270